

ISSN: (Print) (Online) Journal homepage: <https://www.tandfonline.com/loi/tbsd20>

An in-silico investigation based on molecular simulations of novel and potential brain-penetrant GluN2B NMDA receptor antagonists as anti-stroke therapeutic agents

Mohamed El fadili, Mohammed Er-rajy, Wafa Ali Eltayb, Mohammed Kara, Hamada Imtara, Sara Zarougui, Nawal Al-Hoshani, Abdullah Hamadi & Menana Elhallaoui

To cite this article: Mohamed El fadili, Mohammed Er-rajy, Wafa Ali Eltayb, Mohammed Kara, Hamada Imtara, Sara Zarougui, Nawal Al-Hoshani, Abdullah Hamadi & Menana Elhallaoui (2023): An in-silico investigation based on molecular simulations of novel and potential brain-penetrant GluN2B NMDA receptor antagonists as anti-stroke therapeutic agents, Journal of Biomolecular Structure and Dynamics, DOI: [10.1080/07391102.2023.2232024](https://doi.org/10.1080/07391102.2023.2232024)

To link to this article: <https://doi.org/10.1080/07391102.2023.2232024>



Published online: 10 Jul 2023.



Submit your article to this journal [↗](#)




View related articles [↗](#)



View Crossmark data [↗](#)



An in-silico investigation based on molecular simulations of novel and potential brain-penetrant GluN2B NMDA receptor antagonists as anti-stroke therapeutic agents

Mohamed El fadili^a , Mohammed Er-raiy^a, Wafa Ali Eltayb^b, Mohammed Kara^c, Hamada Imtara^d, Sara Zarougui^a, Nawal Al-Hoshani^e, Abdullah Hamadi^f and Menana Elhallaoui^a

^aLIMAS Laboratory, Faculty of Sciences Dhar El Mehraz, Sidi Mohammed Ben Abdellah University, Fez, Morocco; ^bBiotechnology Department, Faculty of Sciences and Technology, Shendi University, Shendi, Sudan; ^cLaboratory of Biotechnology, Conservation and Valorisation of Natural Resources, Faculty of Sciences Dhar El Mehraz, Sidi Mohammed Ben Abdellah University, Fez, Morocco; ^dFaculty of Arts and Sciences, Arab American University Palestine, Jenin, Palestine; ^eDepartment of Biology, College of Science, Princess Nourah bint Abdulrahman University, Riyadh, Saudi Arabia; ^fDepartment of Medical Laboratory Technology, Faculty of Applied Medical Sciences, University of Tabuk, Tabuk, Saudi Arabia

Communicated by Ramaswamy H. Sarma

ABSTRACT

GluN2B-induced activation of NMDA receptors plays a key function in central nervous system (CNS) disorders, including Parkinson, Alzheimer, and stroke, as it is strongly involved in excitotoxicity, which makes selective NMDA receptor antagonists one of the potential therapeutic agents for the treatment of neurodegenerative diseases, especially stroke. The present study aims to examine a structural family of thirty brain-penetrating GluN2B N-methyl-D-aspartate (NMDA) receptor antagonists, using virtual computer-assisted drug design (CADD) to discover highly candidate drugs for ischemic strokes. Initially, the physicochemical and ADMET pharmacokinetic properties confirmed that C13 and C22 compounds were predicted as non-toxic inhibitors of CYP2D6 and CYP3A4 cytochromes, with human intestinal absorption (HIA) exceeding 90%, and designed to be as efficient central nervous system (CNS) agents due to the highest probability to cross the blood-brain barrier (BBB). Compared to ifenprodil, a co-crystallized ligand complexed with the transport protein encoded as 3QEL.pdb, we have noticed that C13 and C22 chemical compounds were defined by good ADME-Toxicity profiles, meeting Lipinski, Veber, Egan, Ghose, and Muegge rules. The molecular docking results indicated that C22 and C13 ligands react specifically with the amino acid residues of the NMDA receptor subunit GluN1 and GluN2B. These intermolecular interactions produced between the candidate drugs and the targeted protein in the B chain remain stable over 200 nanoseconds of molecular dynamics simulation time. In conclusion, C22 and C13 ligands are highly recommended as anti-stroke therapeutic drugs due to their safety and molecular stability towards NMDA receptors.

ARTICLE HISTORY

Received 29 March 2023
Accepted 27 June 2023

KEYWORDS

NMDA; CNS; CADD; ADMET; BBB; molecular docking; molecular dynamics

1. Introduction

According to the 2015 Global Burden of Disease (GBD) report, strokes were classified as the second most common cause of death and the third major cause of disability in the world (Katan & Luft, 2018). Ischemic strokes make up about 87% of all strokes and include oxidative stress, energy failure, apoptosis, brain edema, high-frequency amino acid neurotoxins, and intracellular calcium overload (Barthels & Das, 2020; Reeves et al., 2008). The present study was performed using a virtual screening of a set of thirty brain-penetrant GluN2B NMDAR antagonists, which were previously designed, and biologically evaluated as anti-stroke therapeutic agents, with the help of pharmacophore-merging strategy, through the combination of popular GluN2B ligands and 3-n-Butylphthalide (NBP) structures (Xu et al., 2022). Nowadays, computer-assisted drug design (CADD) based on *in-silico*

techniques has gained great importance and has been largely reported in the literature (El fadili, Er-raiy, et al., 2022; El fadili, Er-Rajy, et al., 2022; Er-raiy, El fadili, Imtara, et al., 2023; Er-raiy, Fadili, et al., 2023; Radan et al., 2022). In this regard, we have examined GluN2B NMDAR antagonists, through the use of computer-assisted drug design (CADD) technology, to detect and identify non-toxic, highly effective CNS agents, intended to be the best anti-stroke therapeutic drugs. During the first part of this work, we examined all thirty NMDA receptor antagonists, using the BOILED-Egg as an accurate predictive model, highly practical in medicinal chemistry to discover the candidate drugs (Daina & Zoete, 2016). Thereafter, we predicted the physicochemical and pharmacokinetic properties of thirty compounds compared to ifenprodil as a co-crystallized ligand complexed to amino-terminal domains of the NMDA receptor subunit GluN1 and GluN2B, encoded as 3QEL.pdb (Bank, n.d.)

(<https://www.rcsb.org/structure/3QEL>), and we assessed their similarity to drugs with the assistance of bioavailability radars, taking into account the evaluation of six important parameters for the design of orally administered drugs, like lipophilicity, polarity, size, solubility, saturation, and flexibility (Daina et al., 2017; Ritchie et al., 2011). In the second part, the molecular docking simulation was performed to explore the intermolecular interactions produced between the transport protein of 3QEL.pdb code, and the most active compounds scored as C13, C22, and C23 which were experimentally defined by the highest level of neuroprotective activity (survival rate of 81.91%, 89.80%, and 88.35%, respectively), meeting the five rules of Lipinski, and the bioavailability conditions of Veber, Egan, Muegge, and Ghose, with a good ADME-Tox profile (El fadili et al., 2023). Thereafter, the molecular mechanics with generalized born and surface area (MMGBSA) solvation was conducted to calculate the binding free energies of three studied complexes (Faisal et al., 2022; Ononamadu et al., 2021). Then, the conformational changes of each complex were examined during 200 nanoseconds of simulation time, with the help of the molecular dynamics technique, a successful technology widely applied to examine the stability of chemical interactions obtained by molecular docking, studying the behavior of proteins towards small molecules with atomic precision and detailed temporal resolution (Hollingsworth & Dror, 2018; Hu et al., 2023). In the last step, the stability and reactivity of candidate drugs was also examined using the density functional theory (DFT) to discover the most powerful drug candidate for the treatment of ischemic stroke (Alameen et al., 2022; Zothantluanga et al., 2023).

2. Materials and methods

2.1. Experimental database

The current study was carried out on thirty brain-penetrating GluN2B N-methyl-D-aspartate (NMDA) receptor antagonists, which were experimentally synthesized through the pharmacophore-merging strategy. This experimental study which was performed by Qinlong Xu et al. in China concluded that about half of 3-ethylisobenzofuran-1(3H)-one derivatives

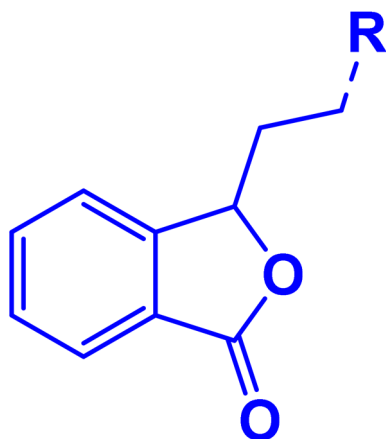


Figure 1. Structural formula of 3-ethylisobenzofuran-1(3H)-one derivatives.

(Figure 1) presented a superior neuroprotective activity to 3-n-butylphthalide (NBP) against NMDA-induced neurotoxicity in hippocampal neurons at 10 μ M, as displayed in Table 1, and also concluded that the chemical compound C22 merits further functional evaluation as novel anti-stroke therapeutic agent (Xu et al., 2022). For this reason, we have examined this experimental database using machine learning techniques, based on ADME and toxicity predictions, drug kinetics assessments, molecular docking, molecular dynamics simulations, and DFT studies to verify the toxicity, ADME pharmacokinetics properties, and stability of intermolecular interactions produced towards the targeted protein.

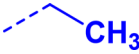
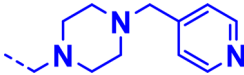
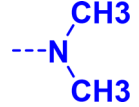
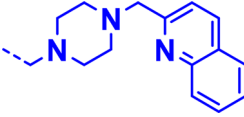
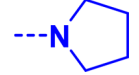
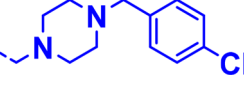
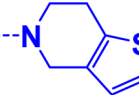
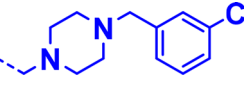
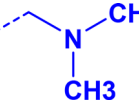
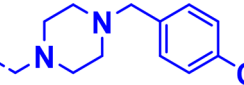
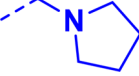
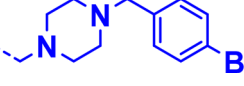
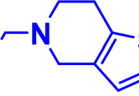
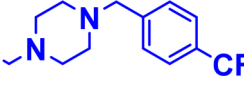
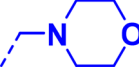
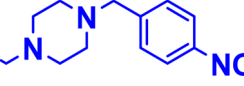
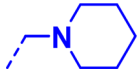
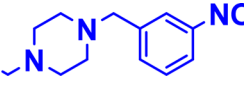
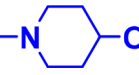
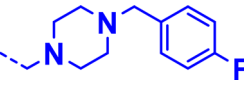
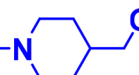
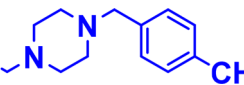
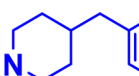
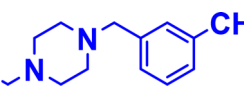
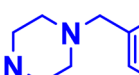
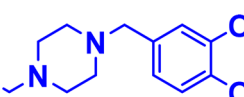
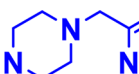
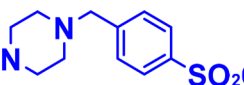
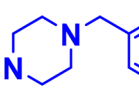
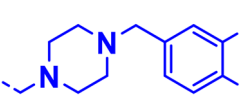
2.2. In-silico pharmacokinetics, drug-likeness, and ADME-toxicity prediction

A certain number of conditions must be satisfied before a drug can be approved for clinical trials. Initially, the BOILED-Egg model based on the calculation of lipophilicity given by the logarithm of the partition coefficient between n-octanol and water ($\text{Log } P_{O/W}$) and polarity signaled by the topological polar surface area (TPSA) of small molecules was applied to identify the potent central nervous system (CNS) agents, with the highest probability to cross the blood-brain barrier (BBB) (Daina et al., 2014; Daina & Zoete, 2016). Secondly, the bioavailability radars were also evaluated on this set of molecules to assess their similarity to drugs meeting the oral bioavailability, considering six molecular descriptors as: lipophilicity, polarity, size, solubility, saturation, and flexibility (Daina et al., 2017; Kandsi et al., 2022; Martin, 2005). Moreover, the physicochemical properties of each compound were studied in the basis of Lipinski (Lipinski et al., 1997), Egan (Egan et al., 2000; Egan & Lauri, 2002), Veber (Veber et al., 2002), Muegge (Muegge, 2003), and Ghose (Yalcin, 2020) rules. Finally, the pharmacokinetic properties of absorption, distribution, metabolism, excretion, and toxicity (ADME-Tox) were predicted and compared to the ADME-Tox profile of ifenprodil as a selective NMDA receptor antagonist, with the help of the online SwissADMET (<http://www.swissadme.ch/>) and pkCSM (<https://biosig.lab.uq.edu.au/pkcsm/prediction>) servers (Daina et al., 2017; PkCSM, n.d.).

2.3. Molecular docking

Molecular docking is an efficient and successful tool for drug discovery (Bassani et al., 2022; El fadili et al., 2023). It's largely applied in the literature to explore the binding affinity and the type of intermolecular interactions produced between the candidate drug and targeted protein (El fadili, Er-rajy, et al., 2022; El fadili, Er-Rajy, et al., 2022; Er-rajy, El fadili, Mujwar, et al., 2023; Er-rajy et al., 2022; Er-Rajy et al., 2022). For this purpose, we extracted the experimentally-determined 3D structure of the N-methyl-D-aspartate (NMDA) receptor from the protein data bank (PDB) archive. The crystal structure of this transport protein encoded as 3QEL.pdb was discovered using the X-RAY diffraction method with a resolution of 2.60 Å (Bank, n.d.) (<https://www.rcsb.org/structure/3QEL>). Then, we prepared our protein using the

Table 1. Neuroprotection of thirty chemical compounds against NMDA-induced neurotoxicity in hippocampal neurons at 10 μ M.

Compounds number	R	Survival rate (%)	Compounds number	R	Survival rate (%)
C1		73.45	C16		75.54
C2		73.56	C17		62.96
C3		70.66	C18		60.33
C4		66.05	C19		62.96
C5		78.18	C20		60.33
C6		73.16	C21		46.13
C7		66.52	C22		89.80
C8		76.22	C23		88.35
C9		77.85	C24		73.28
C10		77.13	C25		72.2
C11		78.14	C26		68.38
C12		79.12	C27		67.43
C13		81.91	C28		48.44
C14		74.65	C29		61.02
C15		63.33	C30		75.45

Discovery Studio 2021 (BIOVIA) package software (BIOVIA Discovery Studio 2021 Client. Get the software safely and easily, n.d.), deleting the water molecules, ion sodium, ifenprodil, and all other co-crystallized ligands linked to protein. Moreover, the Gasteiger charges were computed and the

polar hydrogens were added to improve the cavity performance. So, the prepared protein was docked to C13, C22, and C23 compounds as three most active ligands, using AutoDock 4.2.6/AutoDockTools 1.5.6 software (AutoDock 4.2.6/AutoDockTools 1.5.6—Suite of Automated Docking

Tools—My Biosoftware—Bioinformatics Softwares Blog, n.d.; Norgan et al., 2011). With the help of AUTOGRID algorithm, we centralized the grid box on (81.43 Å, 15.25 Å, -21.157 Å),

putting the sizes: (100, 100, 100) in the 3D structure of (candidate ligand—3QEL.pdb protein) complex, and executing 10 genetic algorithms of a maximum number of evals equal to

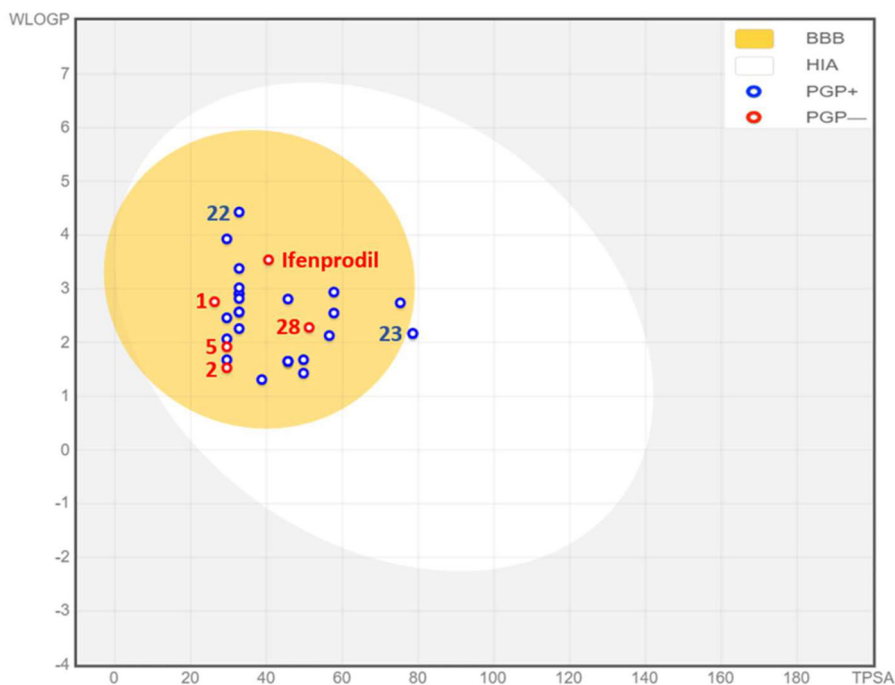


Figure 2. BOILED-Egg model of thirty inhibitors and ifenprodil as co-crystallized ligand.

Table 2. Physicochemical properties of ifenprodil and thirty GluN2B N-methyl-D-aspartate (NMDA) receptor antagonists, based on Lipinski, Veber, Egan, and Ghose violations.

N Rule	Physico-chemical properties						Lipinski	Veber	Egan	Ghose	Muegge
	Molecular weight (g/mol) ≤ 500	Molar refractive index $40 \leq MR \leq 130$	Rotatable bonds < 10	Log P < 5	H-BA ≤ 10	H-BD < 5	violations	violations	violations	violations	violations
							Categorical (Yes/No)				
							Yes/No	Yes/No	Yes/No	Yes/No	Yes/No
C1	190.24	54.99	3	2.53	2	0	Yes	Yes	Yes	Yes	No
C2	205.25	57.89	3	2.39	3	0	Yes	Yes	Yes	Yes	Yes
C3	231.29	69.31	3	2.66	3	0	Yes	Yes	Yes	Yes	Yes
C4	299.39	87.02	3	2.95	3	3	Yes	Yes	Yes	Yes	Yes
C5	219.28	62.70	4	2.64	3	0	Yes	Yes	Yes	Yes	Yes
C6	245.32	74.11	4	2.82	3	0	Yes	Yes	Yes	Yes	Yes
C7	313.41	91.83	4	3.13	3	0	Yes	Yes	Yes	Yes	Yes
C8	261.32	75.20	4	2.72	4	0	Yes	Yes	Yes	Yes	Yes
C9	259.34	78.92	4	3.03	3	0	Yes	Yes	Yes	Yes	Yes
C10	275.34	80.08	4	2.64	4	1	Yes	Yes	Yes	Yes	Yes
C11	289.37	84.89	5	2.82	4	1	Yes	Yes	Yes	Yes	Yes
C12	349.47	108.21	6	3.80	3	0	Yes	Yes	Yes	Yes	Yes
C13	350.45	110.22	6	3.67	4	0	Yes	Yes	Yes	Yes	Yes
C14	351.44	108.01	6	3.42	5	0	Yes	Yes	Yes	Yes	Yes
C15	351.44	108.01	6	3.31	5	0	Yes	Yes	Yes	Yes	Yes
C16	351.44	108.01	6	3.36	5	0	Yes	Yes	Yes	Yes	Yes
C17	401.50	125.52	6	3.98	5	0	Yes	Yes	Yes	Yes	Yes
C18	375.46	114.93	6	3.66	5	0	Yes	Yes	Yes	Yes	Yes
C19	384.90	115.23	6	3.98	4	0	Yes	Yes	Yes	Yes	Yes
C20	384.90	115.23	6	4.05	4	0	Yes	Yes	Yes	Yes	Yes
C21	429.35	117.92	6	4.09	4	0	Yes	Yes	Yes	Yes	Yes
C22	418.45	115.22	7	4.03	7	0	Yes	Yes	Yes	Yes	Yes
C23	395.45	119.04	7	3.45	6	0	Yes	Yes	Yes	Yes	Yes
C24	395.45	119.04	7	3.46	6	0	Yes	Yes	Yes	Yes	Yes
C25	368.44	110.18	6	3.81	5	0	Yes	Yes	Yes	Yes	Yes
C26	364.48	115.18	6	3.66	4	0	Yes	Yes	Yes	Yes	Yes
C27	364.48	115.18	6	3.65	4	0	Yes	Yes	Yes	Yes	Yes
C28	410.51	123.20	8	4.10	6	0	Yes	Yes	Yes	Yes	Yes
C29	428.54	123.31	7	3.35	6	0	Yes	Yes	Yes	Yes	Yes
C30	386.43	110.13	6	3.89	6	0	Yes	Yes	Yes	Yes	Yes
Ifenprodil	323.43	101.49	5	3.47	3	1	Yes	Yes	Yes	Yes	Yes

25000000 for each complex. Lastly, the intermolecular interactions resulting from the strongest complexes with the lowest binding energies in Kcal/mol were visualized using Discovery Studio 2021 software (El fadili, Er-rajy, et al., 2022).

2.4. Molecular dynamics

To assess the level of molecular recognition of the candidate drug, we evaluated its molecular behavior towards the protein target, using the molecular dynamics technique performed by the use of Desmond software, a package from Schrödinger LLC (Drug Discovery | Schrödinger, n.d.). For this goal, the output files of molecular docking were selected as input files of molecular dynamics, to verify the stability of the (C13, C22, C23 ligands—3QEL.pdb protein) complexes, during 200 nanoseconds of molecular dynamics (MD) simulation time. Initially, the studied complexes were prepared using Protein Preparation Maestro and further optimized in the System Builder tool utilizing of the transferable interaction potential 3-point (TIP3P) solvent model, with an OPLS-type force field (Kaminski et al., 2001). Subsequently, the adopted models were neutralized by the addition of the counter ions and water molecules to reproduce the physiological environment of 0.15 M salt (Na⁺, Cl⁻), with a pressure of 1 atm and a temperature of 300 K. Finally, the conformational changes of root mean square fluctuation (RMSF), root

mean square deviation (RMSD), polar surface area (PSA), solvent accessible surface area (SASA), radius of gyration (Rg), and molecular surface area (MolSA) were all registered at 200 nanoseconds of molecular dynamics simulation time (Abdalla & Rabie, 2023; Eltayb et al., 2023).

3. Results and discussion

3.1. Drug kinetics assessment, drug-likeness, and ADME-toxicity profile analysis

The BOILED-Egg model has been applied on thirty antagonists of GluN2B N-methyl-D-aspartate receptor (NMDAR), which have been compared to ifenprodil, as a noncompetitive antagonist of this receptors type, known earlier thanks to its neuroprotective activity against hypertension (Karakas et al., 2011). The results presented in Figure 2, indicate that all the studied compounds are part of the yellow Egan eggs, except compound 23 which is part of the white eggs. Thus, compound 23 belonging to the white region of the egg, has the highest probability of being absorbed from the gastrointestinal tract, and all other compounds have the highest probability to cross the blood-brain barrier (BBB). The chemical compounds C1, C2, C5, C28, and ifenprodil ligand are marked in red, showing that they are predicted not to be effluated from the central nervous system (CNS) by the

Table 3. ADMET *in-silico* pharmacokinetic properties of ifenprodil and thirty GluN2B N-methyl-D-aspartate (NMDA) receptor antagonists.

N	Absorption Intestinal Absorption (Human) Numeric (% Absorbed)	Distribution		Metabolism						Excretion Total Clearance Numeric (Log ml/min/kg)	Toxicity			
		BBB permeability Numeric (Log BB)	CNS Permeability Numeric (LogPS)	Substrate		Inhibitor					AMES toxicity	Hepatotoxicity	Skin Sensitization	
				2D6	3A4	Cytochromes								
						1A2	2C19	2C9	2D6					3A4
C1	95.198	0.237	-1.911	No	No	Yes	No	No	No	No	0.808	No	Yes	Yes
C2	95.246	0.226	-1.93	No	No	No	No	No	No	No	0.992	No	No	Yes
C3	94.194	0.241	-2.16	No	Yes	No	No	No	Yes	No	1.202	No	Yes	Yes
C4	91.909	0.298	-1.208	No	Yes	No	No	No	Yes	No	-1.208	Yes	No	No
C5	94.646	0.3	-1.886	No	Yes	Yes	No	No	Yes	No	0.996	No	Yes	Yes
C6	93.66	0.27	-2.106	No	Yes	No	No	No	Yes	No	1.25	No	Yes	Yes
C7	91.335	0.327	-1.268	No	Yes	No	No	No	Yes	No	1.461	No	No	No
C8	94.975	0.13	-2.201	No	Yes	No	No	No	No	No	1.248	No	Yes	Yes
C9	93.271	0.257	-2.152	No	Yes	No	No	No	Yes	No	1.205	No	Yes	Yes
C10	92.782	0.088	-2.499	No	Yes	No	No	No	No	No	1.188	No	No	No
C11	92.312	0.056	-2.53	No	Yes	No	No	No	Yes	No	1.082	No	No	No
C12	93.056	0.464	-1.195	Yes	Yes	No	No	No	Yes	No	1.133	No	Yes	No
C13	92.838	0.266	-1.145	Yes	Yes	No	No	No	Yes	No	1.142	No	Yes	No
C14	94.803	0.127	-1.995	No	Yes	No	No	No	Yes	Yes	1.159	No	Yes	No
C15	95.02	0.135	-1.832	No	Yes	No	No	No	Yes	No	1.129	No	Yes	No
C16	95.048	0.135	-1.832	No	Yes	No	No	No	Yes	No	1.162	No	Yes	No
C17	92.643	0.25	-1.419	Yes	Yes	Yes	No	No	Yes	No	1.162	No	Yes	No
C18	93.001	0.013	-2.164	Yes	Yes	No	No	No	Yes	No	1.16	No	Yes	No
C19	91.984	0.268	-1.309	Yes	Yes	No	No	No	Yes	No	1.022	No	Yes	No
C20	91.492	0.316	-1.392	Yes	Yes	No	No	No	Yes	Yes	1.065	No	Yes	No
C21	91.425	0.314	-1.392	Yes	Yes	No	No	No	Yes	Yes	1.045	No	Yes	No
C22	90.338	0.283	-1.36	Yes	Yes	No	No	No	Yes	Yes	0.917	No	Yes	No
C23	92.104	-0.345	-2.383	Yes	Yes	No	No	No	Yes	No	0.83	Yes	Yes	No
C24	92.137	-0.293	-2.378	Yes	Yes	No	No	No	No	Yes	0.824	Yes	Yes	No
C25	92.394	0.309	-1.418	Yes	Yes	No	No	No	Yes	Yes	1.026	No	Yes	No
C26	92.95	0.329	-1.392	Yes	Yes	No	No	No	Yes	Yes	1.078	No	Yes	No
C27	93.442	0.281	-1.309	Yes	Yes	No	No	No	Yes	No	1.051	No	Yes	No
C28	93.179	0.223	-2.52	Yes	Yes	No	No	No	Yes	Yes	1.117	No	Yes	No
C29	94.23	0.021	-2.624	No	Yes	No	No	No	No	No	0.944	No	Yes	No
C30	91.635	0.301	-1.43	Yes	Yes	No	No	No	Yes	Yes	1.002	No	Yes	No
Ifenprodil	92.417	0.046	-1.079	Yes	Yes	Yes	No	No	Yes	No	0.993	No	No	No

P-glycoprotein. Inversely, all other compounds colored in bleu, are predicted to be successfully evacuated from the CNS by the P-glycoprotein except molecule 23, because it is most likely to be passively absorbed by the gastrointestinal tract (Daina & Zoete, 2016).

Moreover, the predicted physicochemical properties of thirty GluN2B N-methyl-D-aspartate (NMDA) receptor antagonists, were compared to ifenprodil, based on five rules of Lipinski, and the violations number of Veber, Egan, Ghose,

and Muegge. The results presented in Table 2, demonstrate that GluN2B NMDA receptor antagonists satisfy all five rules of Lipinski, where: molecular weight (MW) ≤ 500 , $40 \leq$ molar refractivity (MR) ≤ 130 , Log P (octanol/water) < 5 , hydrogen bond acceptor (HBA) ≤ 10 , and hydrogen bond donor (HBD) < 5 . Then, the bioavailability number of Veber, Egan, Ghose, and Muegge is successfully verified, except for compound C1, which didn't satisfy the Muegge rule, because it's defined by a molecular weight inferior to 200 g/mol.



Figure 3. Bioavailability radars of ifenprodil and thirty compounds, taking into account six physicochemical properties ideal for oral bioavailability, namely lipophilicity (LIPO), polarity (POLAR), size (SIZE), solubility (INSOLU), saturation (INSATU), and flexibility (FLEX).

The pharmacokinetic properties of absorption, distribution, metabolism, excretion, and toxicity (ADME-Tox) of thirty molecules, were also compared to the ADMET profile of ifenprodil, as resulted in Table 3. We have recorded that all thirty GluN2B NMDA receptor antagonists and a noncompetitive antagonist of NMDA receptors (ifenprodil) are characterized by very good human intestinal absorption (HIA superior to 90%), and defined by blood-brain barrier (BBB) permeabilities superior to -1 Log BB, and central nervous system (CNS) permeabilities included between -1 and -3 Log PS. In

addition, they are predicted as inhibitors of CYP1A2, CYP2D6, and CYP3A4 cytochromes, but they have any effect on CYP2C9 and CYP2C19 cytochromes. All chemical compounds are predicted by similar excretion, which is defined by a total clearance that does not decrease by 0.8 log ml/min/kg, except for C4 compound (total clearance of -1.208 log ml/min/kg). The AMES toxicity test indicates that all GluN2B NMDA receptor antagonists are predicted as not toxic inhibitors, except C4, C23, and C24 compounds. Most of these compounds do not cause skin sensitization, but they are



Figure 3. Continued

predicted to have significant hepatotoxicity in the human organism, as an adverse side effect like any other medications.

As a result, C4, C23, and C24 compounds were predicted as toxic products, according to the AMES toxicity test. C23 compound was predicted to be absorbed by the gastrointestinal tract, because it's part of white Egan Egg. C1, C2, C5, and C28 ligands are predicted not to be evacuated from the central nervous system (CNS) by the P-glycoprotein. While the majority of the remaining compounds do not cause skin sensitization, but they present marked hepatotoxicity in the human organism. C22 ligand was successfully examined with a good ADMET profile, respecting Lipinski, Veber, Egan, Muegge, and Rhose rules.

Recently, increasing attention has been directed to the necessity of assessing the bioavailability problems of potential drugs. This need was particularly marked for drug discovery projects (Martin, 2005). For this reason, we have examined the bioavailability of ifenprodil and GluN2B N-methyl-D-aspartate receptor antagonists, based on bioavailability radars technology, considering six physicochemical

properties ideally adapted for oral bioavailability, namely lipophilicity, polarity, size, solubility, saturation, and flexibility. Where, lipophilicity (LIPO): $-0.7 < XLOGP3 < +5$, SIZE: $150 < MV < 500$ g/mol, polarity (POLAR): $20 \text{ \AA}^2 < TPSA < 130 \text{ \AA}^2$, insolubility (INSOLU): $-6 < LOG S < 0$, insaturation (INSATU): $0.25 < \text{Fraction Csp3} < 1$, and flexibility (FLEX): $0 < \text{Number of rotatable bonds} < 9$. The pink-colored area is the suitable physicochemical space for oral bioavailability, in which the graph of each molecule must be fully adjusted to be declared as drug-like (Kandsi et al., 2022). The present study shows that all compounds adhere to the suitable space for oral bioavailability because they are part of the pink zone of bioavailability radars without exception, as displayed in Figure 3.

3.2. Molecular docking simulation

2D and 3D visualizations of molecular docking resulted in Figure 4, show that the C22 compound reacts specifically with Gln 152, Lys 382, Trp 379, Tyr 282, and Lys 361 amino acid residues of 3QEL.pdb protein with a binding energy of

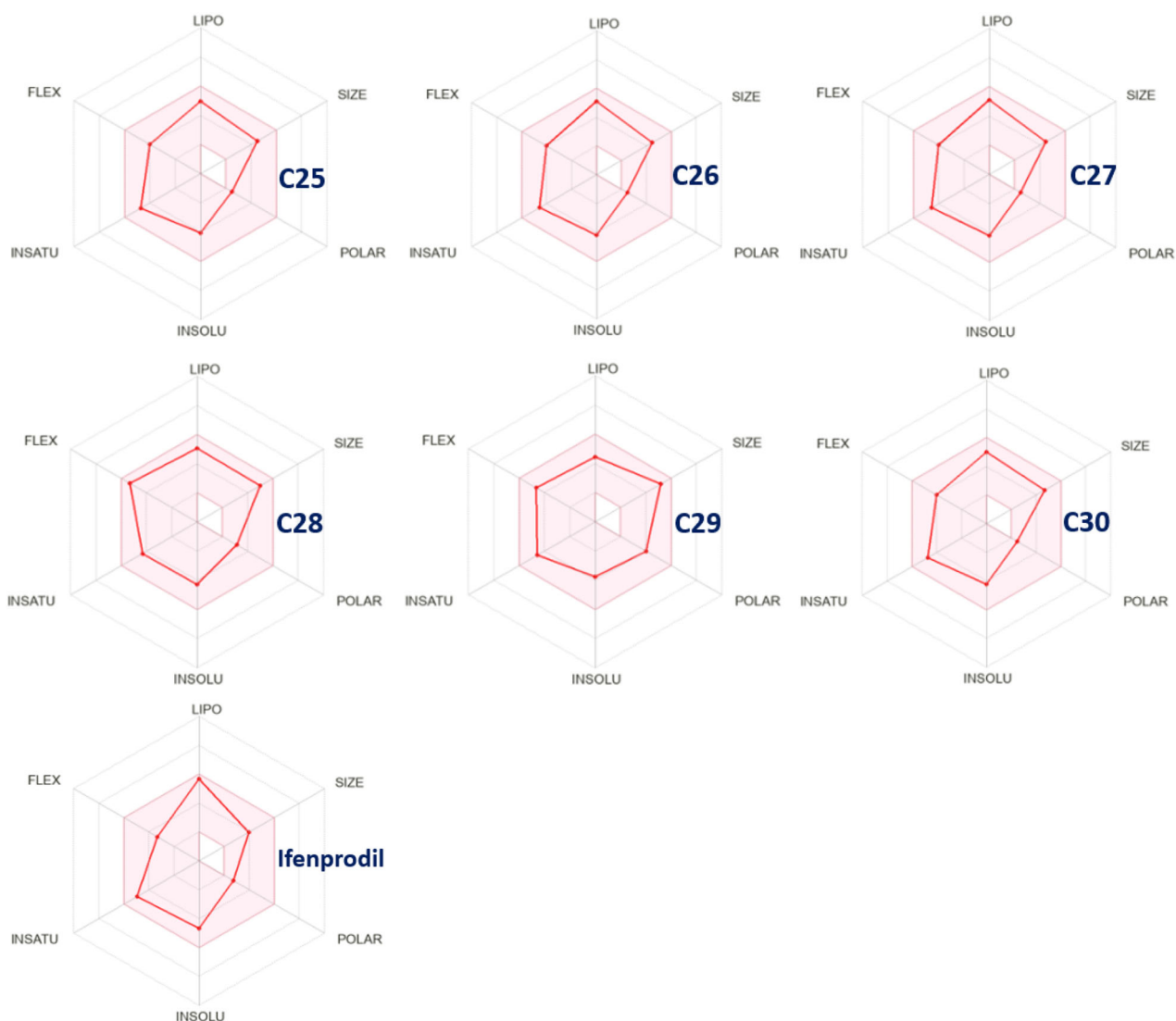


Figure 3. Continued

-7.27 kcal/mol, creating five conventional hydrogen bonds, with nuclear distances of 2.29 Å, 2.67 Å, 2.20 Å, 2.03 Å, and 2.82 Å, respectively. Three first conventional hydrogen bonds were produced with fluorine atoms, and last two were created with oxygen atom of ketonic function. This type of intermolecular interaction makes the C22 ligand so stable toward the targeted protein. In addition, one carbon

hydrogen bond was produced with Pro 360 amino acid residue, and two Pi-alkyl bonds were formed with Arg 347, and Leu 349 amino acid residues. While, the C13 compound was docked to the targeted protein with a binding energy of -7.89 kcal/mol, producing two hydrogen bonds towards Thr 174 and Thr 233 amino acid residues, with nuclear distances of 3.01 Å, and 3.11 Å, respectively. Then, one Alkyl

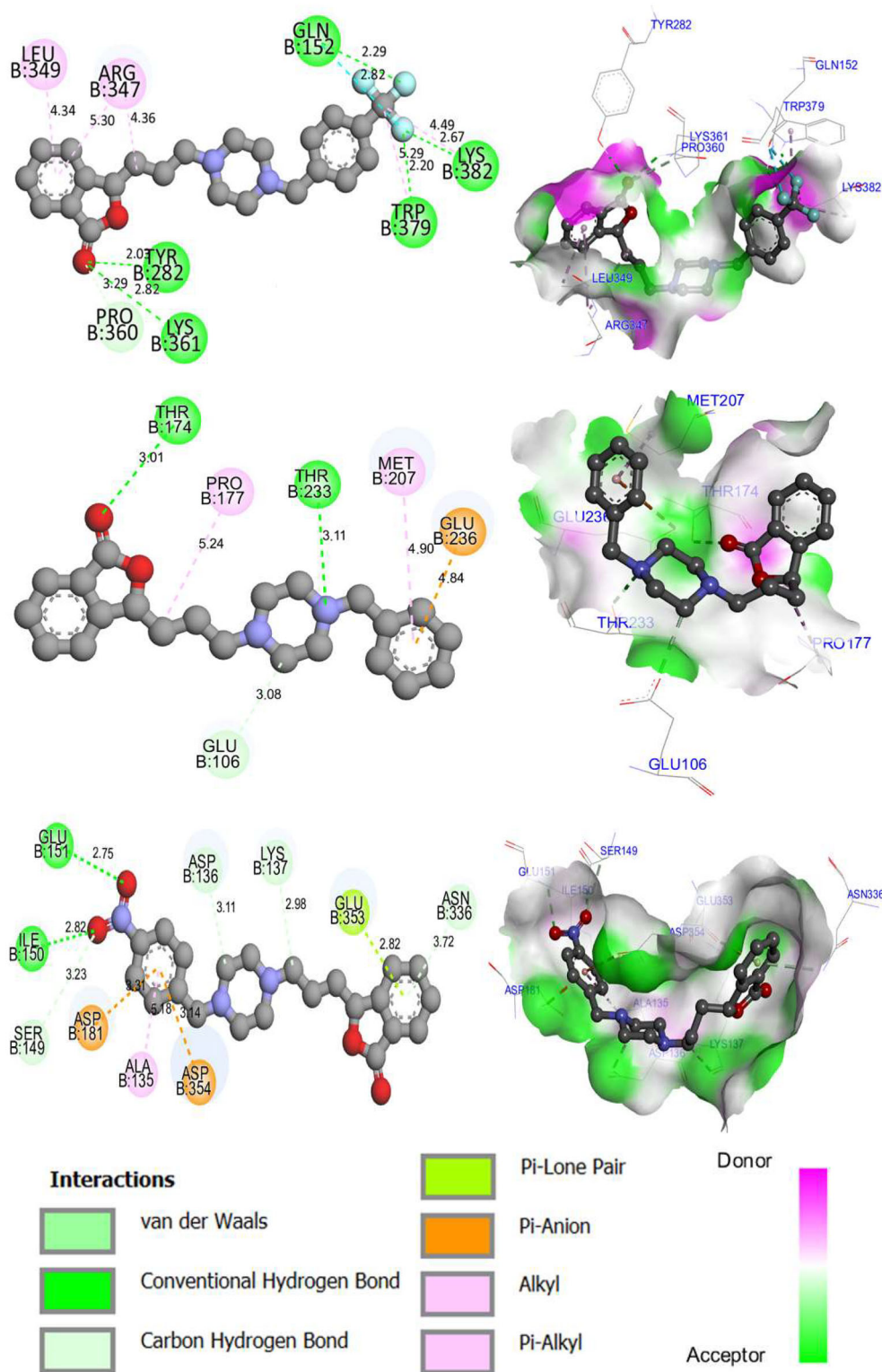


Figure 4. 2D and 3D visualizations of intermolecular interactions established between 3QEL.pdb protein and C22, C13, and C23 ligands, with binding energy of -7.27 kcal/mol, -7.89 kcal/mol, and -9.17 kcal/mol, respectively.

bond was formed with Pro 177 amino acid residue at 5.24 Å, one Pi-Alkyl bond was created with Met 207 amino acid residue at 4.90 Å, and one other Pi-Anion bond was created to Glu 236 amino acid residue at 4.84 Å, and Carbon Hydrogen bond was formed with Glu 106 amino acid residue at 3.08 Å. Concerning the C23 compound, it was docked to the protein target with a binding energy of -9.17 kcal/mol, forming two Hydrogen bonds towards Glu 151, and Ile 150 amino acid residues, with nuclear distances of 2.75 Å, and 2.82 Å, respectively. Moreover, two Pi-Anion bonds were created with Asp 181 and Asp 354 at 3.31 Å and 3.14 Å, respectively. One Pi-Alkyl bond was produced

with Ala 135 amino acid residue at 5.18 Å, and one Pi-Lone Pair bond was formed Glu 353 amino acid residue at 2.82 Å. In addition, four Carbon Hydrogen bonds were produced with Ser 149, Asp 136, Lys 137, and Asn 336 amino acid residues, at 3.23 Å, 3.11 Å, 2.98 Å, and 3.72 Å, respectively. These chemical bonds include intermolecular interactions similar to those detected towards the Glu 236, Pro 177, Met 207, and Glu 106 amino acid residues, which have been found by candidate selective antagonists of the N-Methyl-D-Aspartate (NMDA) receptor subunit 2B, which were designed to treat neuropathic pain, in particular Parkinson's, Huntington's, and Alzheimer's diseases (El fadili,

Table 4. Binding energies in kcal/mol of the studied complexes using MMGBSA approach.

Studied complex	MMGBSA dG Bind	MMGBSA dG Bind Coulomb	MMGBSA dG Bind Covalent	MMGBSA dG Bind Hbond	MMGBSA dG Bind Lipo	MMGBSA dG Bind packing	MMGBSA dG Bind Solv GB	MMGBSA dG Bind vdW
C22 – protein	-68.4791617	-89.4000894	3.587672457	-0.80935759	-24.58127916	-2.529968808	97.4565515	-52.2026907
C13 – protein	-52.2744679	-83.1266545	3.849614219	-0.54666909	-21.03976226	-2.218290244	92.2753436	-41.4680496
C23 – protein	-47.7334229	-113.000573	2.859691276	-1.27631036	-14.30883244	-0.869315669	132.261756	132.261756

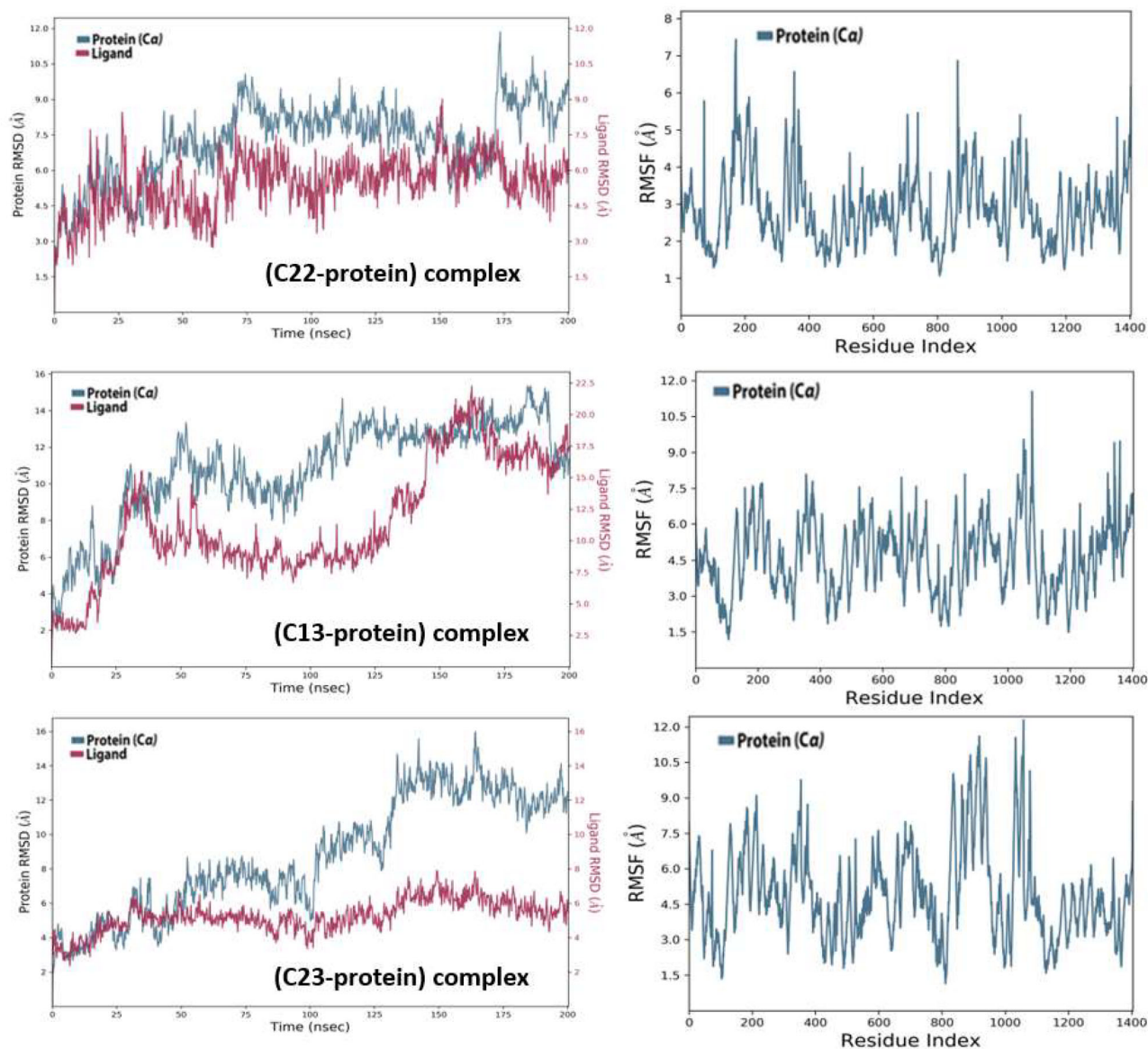


Figure 5. Changes in root mean square deviation (RMSD) and root mean square fluctuation (RMSF) during 200 nanoseconds of molecular dynamics (MD) simulation time for C22, C13, and C23 ligands complexed to 3QEL.pdb protein.

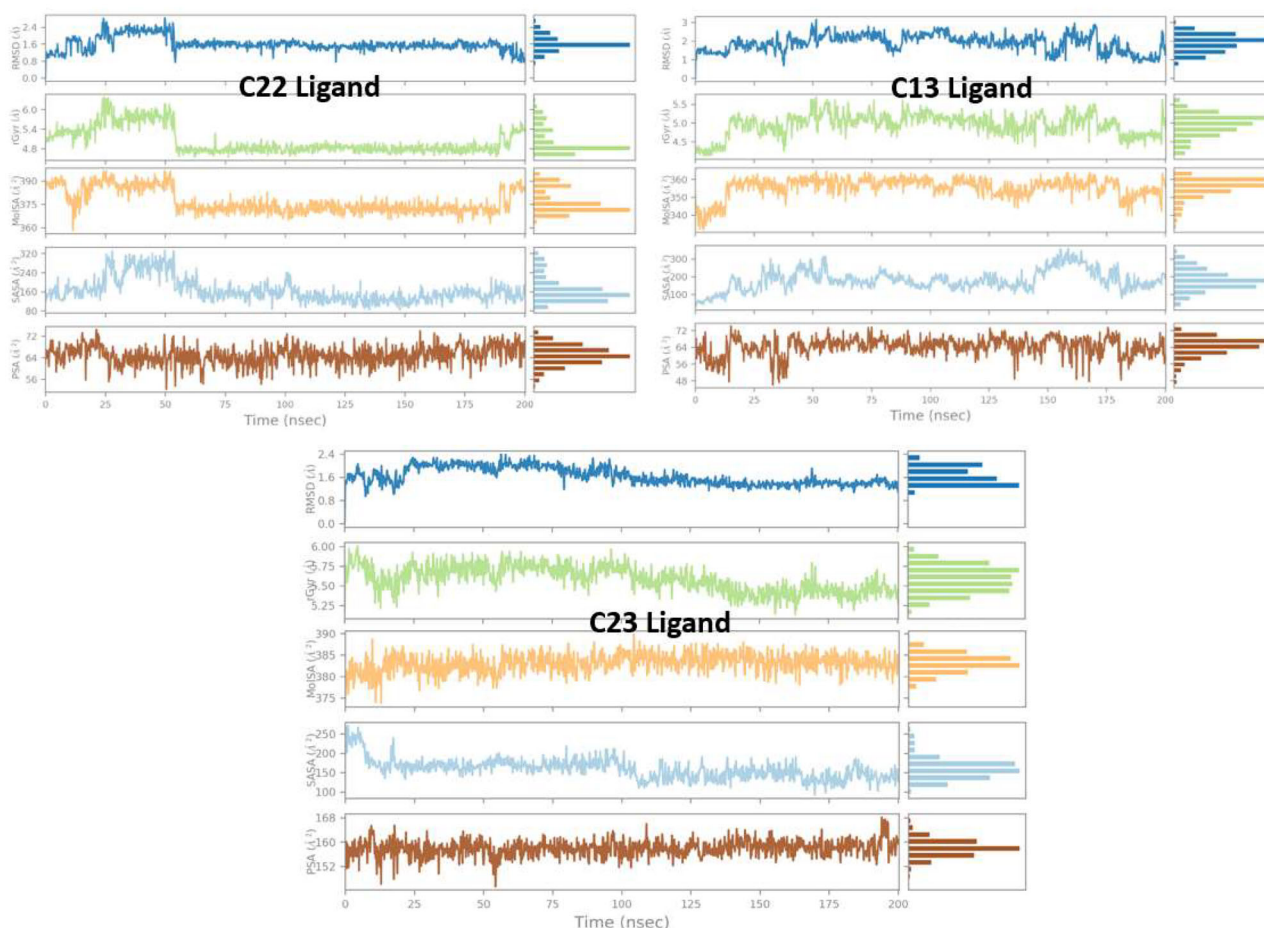


Figure 6. Variations of root mean square deviation (RMSD), radius of gyration (r Gyr), molecular surface area (MoISA), solvent accessible surface area (SASA) and polar surface area (PSA) during 200 ns of MD simulation time for C22, C13, and C23 ligands complexed to 3QEL.pdb protein.

Er-rajy, et al., 2022). The key amino acid residues, namely Glu 236, and Pro 177 from GluN2B subtypes of NMDA receptor were also detected for the most active indoles in complex with the same targeted protein encoded as 3QEL.pdb. As well as, the key residue Glu 236, was equally detected in the same way as the Gln 110 residue for ifenprodil, and Ro 25-6981 as selective and competitive antagonists of NMDA receptors subunit 2B, providing pharmacological therapies for chronic neurodegenerative diseases, in particular Alzheimer, Parkinson, depression, schizophrenia, and neuronal loss after stroke (Buemi et al., 2016; Temme et al., 2018). Therefore, we conclude that the most active ligands labelled C13, C22, and C23 reacted similarly to N-Methyl-D-Aspartate receptors (NMDARs) subunit 2B (3QEL.pdb), producing almost the same intermolecular interactions towards the active sites of the targeted protein. As a result, they could be potential treatments for neurodegenerative disorders, acting in the same way as well-known drugs such as ifenprodil, Ro 25-6981, Tacrine, memantine, and MK-801 (Alhumaydhi et al., 2021; Crismon, 1994; Liu et al., 2020; Sonkusare et al., 2005; Thakral et al., 2023).

3.3. Molecular dynamics simulation

To verify the stability of intermolecular interactions produced between the transport protein encoded as

3QEL.pdb and C22, C13, and C23 compounds, we have performed the molecular dynamics (MD) technique on (targeted protein-candidate drug) complexes during 200 nanoseconds of MD simulation time. The Molecular Mechanics with Generalized Born and Surface Area (MMGBSA) solvation was conducted to calculate the binding free energies of the studied complexes, as resulted in Table 4 (Faisal et al., 2022; Ononamadu et al., 2021). The MMGBSA approach shows that the binding energies are negatively very large, indicating that the candidate ligands have reacted with the protein target with low energies (minimal ΔG Bind scores), which makes the complexes stable with optimal energies during the molecular dynamic's simulation time.

Additionally, the results of conformational changes presented in Figure 5, indicate that root mean square deviation (RMSD) values of C22 compound as pictured in red, were predicted with a good level of molecular stability. Furthermore, the candidate drug does not diffuse further from the targeted protein, as marked in blue, because the ligand still linked to the responsible protein throughout 200 ns of MD simulation time, which mean that the previous interactions produced by molecular docking, render the complex so stable. Additionally, the protein root mean square fluctuation (RMSF) variation shows only two remarkable fluctuations for some protein residue indexes, so all

other fluctuations were estimated to be negligible as they oscillate around the mean fluctuation. Furthermore, the conformational changes corresponding to the C13 and C23 ligands appear almost identical, as the RMSD values oscillated parallel to the protein target during the first fifty nanoseconds, but deviate slightly during the last 50 nanoseconds until the end of the simulation time. Moreover, the RMSF values of the protein target in blue were detected in a small range from 1 Å to 9 Å with negligible fluctuations after being bound to C13 and C23 ligands, similar to C22 compound.

The same observations were reported regarding the conformational changes in the ligands properties as the radius of gyration (r Gyr), molecular surface area (MolSA), solvent accessible surface area (SASA), and polar surface area (PSA), where they seem unstable during some nanoseconds, while they become more stable during the remaining time of the

simulation time, as displayed in Figure 6, which demonstrates that C22, C13, and C23 ligands were very flexible after being bound to 3QEL.pdb protein, with few negligible changes in ligand compactness, due to the contribution of polar atoms such as nitrogen, oxygen, and fluorine elements, which confirms the highest level of molecular stability attained by the (ligand-protein) complexes. Consequently, the stability of intermolecular interactions produced between the candidate drugs and protein target was successfully examined by molecular dynamics technique during 200 nanoseconds of MD simulation time.

3.4. Chemical reactivity using DFT calculations

To examine the stability and chemical reactivity of the most active compounds (C22, C13, and C23), the calculations of Density Functional Theory (DFT) were applied on B3LYP,

Table 5. DFT Calculations for the candidate drugs.

	E. LUMO (eV)	E. HOMO (eV)	ΔE (eV)	χ Pauling	η (eV)	μ (eV)	S	ω (eV)
C22	-0.052845041	-0.2124489	0.159603816	-0.13265	0.079802	0.132647	6.265514	0.110243
C13	-0.051013771	-0.200711	0.149697224	-0.12586	0.074849	0.125862	6.680151	0.105823
C23	-0.081295983	-0.2015935	0.120297517	-0.14144	0.060149	0.141445	8.312724	0.166309

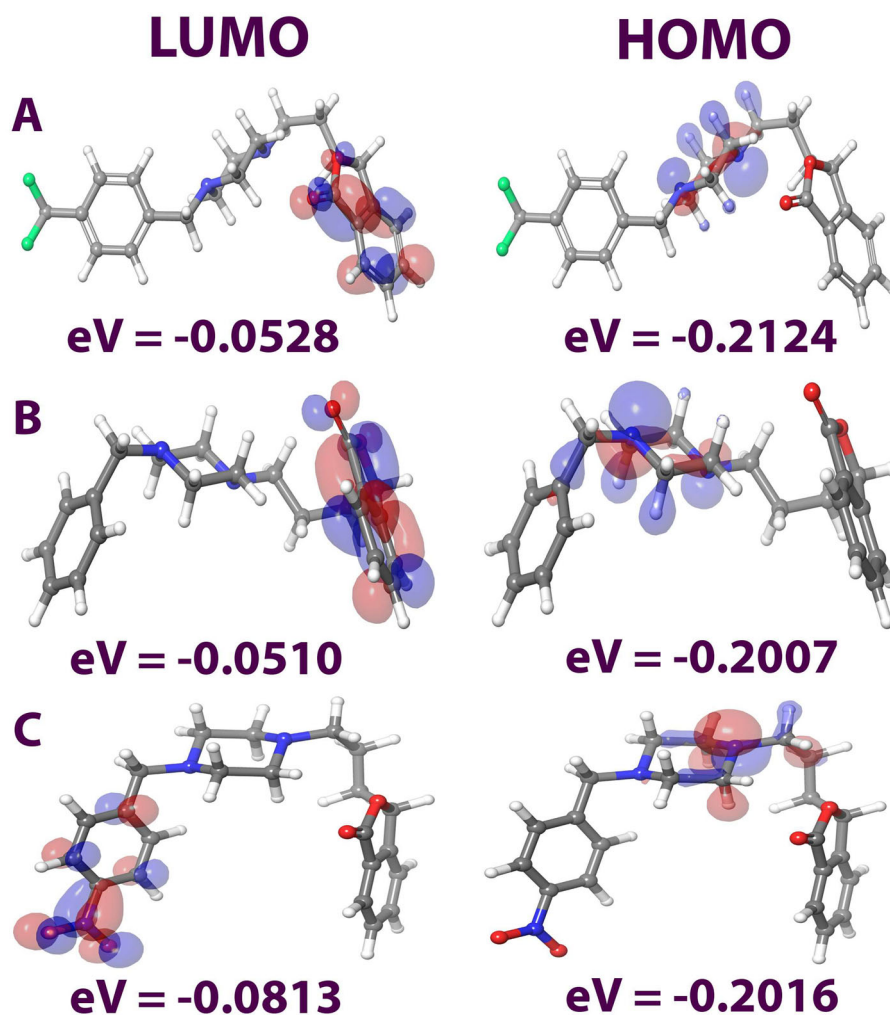


Figure 7. Frontier molecular orbitals (FMO) of the most active compounds C22 (A), C13 (B), and C23 (C).

6–31 + G (d, p) basis. The results of DFT calculations presented in Table 5, summarize all energetic values obtained for the electrostatic descriptors involved in the chemical reactivity of the candidate drugs, as the difference in binding energy [$\Delta E = E. \text{HOMO} - E. \text{LUMO}$], where the chemical compound defined by a lower energy gap corresponds to a higher stability and probably exhibits a high level of reactivity towards the protein target. Moreover, the negative values of Pauling electronegativity (χ), indicate favorable interaction behavior towards the protein target, and positive values of chemical electron potential (μ) display spontaneous chemical reactivity for the candidate molecules. Similarly, the positive values for chemical softness (S) and chemical hardness (η) again confirm the molecular interactions of the candidate drugs. In addition, one other molecular property like electrophilicity index (ω) which explains the ability to accept an electron from the outside environment, especially when expressed positively.

The transfer of electrons that largely contributes to the binding of the candidate compounds with the protein target was presented by the highest occupied molecular orbital (HOMO) and lowest unoccupied molecular orbital (LUMO). For this reason, we focused on the Frontier Molecular Orbitals (FMO) analysis, which was done to identify the most likely reactive sites of the C22, C13, and C23 compounds, as resulted in Figure 7. Where, the red areas represent the attractive potential, while the blue areas represent the repulsive potential, which play an essential role in the chemical reactivity. In addition, the negative values of frontier orbitals confirm the stability of the compound, and the minimal value of gap energies (ΔE) values equal to 0.159603816, 0.149697224, and 0.120297517 for C22, C13, and C23 respectively, which confirm again that most active molecules are so flexible to react with targeted protein, and the reactive sites are in good agreement with the intermolecular interactions resulted in molecular docking simulation (Alameen et al., 2022; Zothantluanga et al., 2023). Therefore, all three molecules could exhibit a stable behavior during their interactions with the targeted protein.

4. Conclusion

The virtual screening adopted in the current study succeeded to predict the toxicity of three molecules marked as C4, C23, and C24 according to the AMES toxicity test, that we do not recommend as therapeutic agents for stroke. In contrast, most of the remaining compounds do not cause skin sensitization, but they present significant hepatotoxicity for the human body. In addition, the C22 and C13 compounds were successfully tested as a non-toxic inhibitor of CYP2D6 and CYP3A4 cytochromes, with a good ADMET profile, and designed to be an efficient central nervous system (CNS) agent due to the highest probability to cross the blood-brain barrier (BBB), meeting the violations number of Egan, Veber, Rhose, and Muegge, and complies with all five Lipinski rules, forming stable intermolecular interactions with the amino acid residues of the transport protein coded as

3QEL.pdb over 200 ns of molecular dynamic (MD) simulation time. Therefore, we strongly recommend the chemical compounds called C22 and C13 as powerful anti-stroke drugs.

CRediT authorship contribution statement

Mohammed El fadili: Conceptualization, Data curation, Formal analysis, Investigation, Methodology, Project administration, Visualization, Writing—original draft, Writing—review & editing. Mohamed Er-rajy, Wafa Eltayeb and Mohammed Kara: Conceptualization, Data curation, Writing—original draft, Writing. Hamada Imtara, Sara Zarougui, Nawal Al-Hoshani, and Abdullah Hamadi: Investigation, Methodology, Writing, review, editing and Investigation. Menana Elhallaoui: Conceptualization, Formal analysis, Methodology, Project administration, Resources, Supervision, Writing—review & editing.

Disclosure statement

No potential conflict of interest was reported by the author(s).

Funding

Princess Nourah bint Abdulrahman University Researchers Supporting Project number [PNURSP2023R437], Princess Nourah bint Abdulrahman University, Riyadh, Saudi Arabia

ORCID

Mohamed El fadili  <http://orcid.org/0000-0002-2211-3298>

References

- Abdalla, M., & Rabie, A. M. (2023). Dual computational and biological assessment of some promising nucleoside analogs against the COVID-19-Omicron variant. *Computational Biology and Chemistry*, 104, 107768. <https://doi.org/10.1016/j.compbiolchem.2022.107768>
- Alameen, A. A., Abdalla, M., Alshibl, H. M., AlOthman, M. R., Alkhulaifi, M. M., Mirgany, T. O., & Elsayim, R. (2022). In-silico studies of glutathione peroxidase4 activators as candidate for multiple sclerosis management. *Journal of Saudi Chemical Society*, 26(6), 101554. <https://doi.org/10.1016/j.jscs.2022.101554>
- Alhumaydhi, F. A., Aljasir, M. A., Aljohani, A. S. M., Alsagaby, S. A., Alwashmi, A. S. S., Shahwan, M., Hassan, M. I., Islam, A., & Shamsi, A. (2021). Probing the interaction of memantine, an important Alzheimer's drug, with human serum albumin: *In silico* and *in vitro* approach. *Journal of Molecular Liquids*, 340, 116888. <https://doi.org/10.1016/j.molliq.2021.116888>
- AutoDock 4.2.6/AutoDockTools 1.5.6 – Suite of Automated Docking Tools – My Biosoftware – Bioinformatics Softwares Blog. (n.d). Retrieved November 19, 2022, from <https://mybiosoftware.com/autodock-4-2-3-autodocktools-1-5-6-suite-automated-docking-tools.html>
- Bank, R. P. D. (n.d.). RCSB PDB – 3QEL: Crystal structure of amino terminal domains of the NMDA receptor subunit GluN1 and GluN2B in complex with ifenprodil. Retrieved June 13, 2023, from <https://www.rcsb.org/structure/3QEL>
- Barthels, D., & Das, H. (2020). Current advances in ischemic stroke research and therapies. *Biochimica et Biophysica Acta. Molecular Basis of Disease*, 1866(4), 165260. <https://doi.org/10.1016/j.bbdis.2018.09.012>
- Bassani, D., Pavan, M., Bolcato, G., Sturlese, M., & Moro, S. (2022). Re-exploring the ability of common docking programs to correctly

- reproduce the binding modes of non-covalent inhibitors of SARS-CoV-2 protease Mpro. *Pharmaceuticals*, 15(2), 180. <https://doi.org/10.3390/ph15020180>
- BIOVIA Discovery Studio 2021 Client. Get the software safely and easily. (n.d.). Software Informer. Retrieved November 19, 2022, from <https://biovia-discovery-studio-2021-client.software.informer.com/>
- Buemi, M. R., De Luca, L., Ferro, S., Russo, E., De Sarro, G., & Gitto, R. (2016). Structure-guided design of new indoles as negative allosteric modulators (NAMs) of N-methyl-D-aspartate receptor (NMDAR) containing GluN2B subunit. *Bioorganic & Medicinal Chemistry*, 24(7), 1513–1519. <https://doi.org/10.1016/j.bmc.2016.02.021>
- Crismon, M. L. (1994). Tacrine: First drug approved for Alzheimer's Disease. *The Annals of Pharmacotherapy*, 28(6), 744–751. <https://doi.org/10.1177/106002809402800612>
- Daina, A., Michielin, O., & Zoete, V. (2014). iLOGP: A simple, robust, and efficient description of *n*-Octanol/water partition coefficient for drug design using the GB/SA approach. *Journal of Chemical Information and Modeling*, 54(12), 3284–3301. <https://doi.org/10.1021/ci500467k>
- Daina, A., Michielin, O., & Zoete, V. (2017). SwissADME: A free web tool to evaluate pharmacokinetics, drug-likeness and medicinal chemistry friendliness of small molecules. *Scientific Reports*, 7(1), 42717. <https://doi.org/10.1038/srep42717>
- Daina, A., & Zoete, V. (2016). A BOILED-Egg to predict gastrointestinal absorption and brain penetration of small molecules. *ChemMedChem*, 11(11), 1117–1121. <https://doi.org/10.1002/cmcd.201600182>
- Drug Discovery | Schrödinger. (n.d.). Retrieved November 19, 2022, from <https://www.schrodinger.com/platform/drug-discovery>
- Egan, W. J., & Lauri, G. (2002). Prediction of intestinal permeability. *Advanced Drug Delivery Reviews*, 54(3), 273–289. [https://doi.org/10.1016/S0169-409X\(02\)00004-2](https://doi.org/10.1016/S0169-409X(02)00004-2)
- Egan, W. J., Merz, K. M., & Baldwin, J. J. (2000). Prediction of drug absorption using multivariate statistics. *Journal of Medicinal Chemistry*, 43(21), 3867–3877. <https://doi.org/10.1021/jm000292e>
- El Fadili, M., Er-Rajy, M., Ali Eltayb, W., Kara, M., Assouguem, A., Saleh, A., Al Kamaly, O., Zerougui, S., & Elhallaoui, M. (2023). In-silico Screening Based on Molecular Simulations of 3,4-disubstituted Pyrrolidine Sulfonamides as Selective and Competitive GlyT1 Inhibitors. *Arabian Journal of Chemistry*, 105105. <https://doi.org/10.1016/j.arabjc.2023.105105>
- El Fadili, M., Er-Rajy, M., Imtara, H., Kara, M., Zarougui, S., Altwajry, N., Al Kamaly, O., Al Sfouk, A., & Elhallaoui, M. (2022). 3D-QSAR, ADME-Tox *in silico* prediction and molecular docking studies for modeling the analgesic activity against neuropathic pain of novel NR2B-selective NMDA receptor antagonists. *Processes*, 10(8), 1462. <https://doi.org/10.3390/pr10081462>
- El Fadili, M., Er-Rajy, M., Imtara, H., Noman, O. M., Mothana, R. A., Abdullah, S., Zerougui, S., & Elhallaoui, M. (2023). QSAR, ADME-Tox, molecular docking and molecular dynamics simulations of novel selective glycine transporter type 1 inhibitors with memory enhancing properties. *Heliyon*, 9(2), e13706. <https://doi.org/10.1016/j.heliyon.2023.e13706>
- El Fadili, M., Er-Rajy, M., Kara, M., Assouguem, A., Belhassan, A., Alotaibi, A., Mrabti, N. N., FIDan, H., Ullah, R., Ercisli, S., Zarougui, S., & Elhallaoui, M. (2022). QSAR, ADMET *in silico* pharmacokinetics, molecular docking and molecular dynamics studies of novel bicyclo (Aryl Methyl) Benzamides as potent GlyT1 inhibitors for the treatment of schizophrenia. *Pharmaceuticals*, 15(6), 670. <https://doi.org/10.3390/ph15060670>
- Eltayb, W. A., Abdalla, M., & Rabie, A. M. (2023). Novel investigational anti-SARS-CoV-2 agent Ensitrelvir "S-217622": A very promising potential universal broad-spectrum antiviral at the therapeutic frontline of coronavirus species. *ACS Omega*, 8(6), 5234–5246. <https://doi.org/10.1021/acsomega.2c03881>
- Er-Rajy, M., El Fadili, M., Hadni, H., Mrabti, N. N., Zarougui, S., & Elhallaoui, M. (2022). 2D-QSAR modeling, drug-likeness studies, ADMET prediction, and molecular docking for anti-lung cancer activity of 3-substituted-5-(phenylamino) indolone derivatives. *Structural Chemistry*, 33(3), 973–986. <https://doi.org/10.1007/s11224-022-01913-3>
- Er-Rajy, M., El Fadili, M., Imtara, H., Saeed, A., Ur Rehman, A., Zarougui, S., Abdullah, S. A., Alahdab, A., Parvez, M. K., & Elhallaoui, M. (2023). 3D-QSAR Studies, molecular docking, molecular dynamic simulation, and ADMET proprieties of novel pteridinone derivatives as PLK1 inhibitors for the treatment of prostate cancer. *Life*, 13(1), 127. <https://doi.org/10.3390/life13010127>
- Er-Rajy, M., El Fadili, M., Mujwar, S., Zarougui, S., & Elhallaoui, M. (2023). Design of novel anti-cancer drugs targeting TRKs inhibitors based 3D QSAR, molecular docking and molecular dynamics simulation. *Journal of Biomolecular Structure and Dynamics*, 0(0), 1–14. <https://doi.org/10.1080/07391102.2023.2170471>
- Er-Rajy, M., El Fadili, M., Mrabti, N. N., Zarougui, S., & Elhallaoui, M. (2022). QSAR, molecular docking, ADMET properties *in silico* studies for a series of 7-propanamide benzoxaboroles as potent anti-cancer agents. *Chinese Journal of Analytical Chemistry*, 50(12), 100163. <https://doi.org/10.1016/j.cjac.2022.100163>
- Er-Rajy, M., Fadili, M. E., Mujwar, S., Lenda, F. Z., Zarougui, S., & Elhallaoui, M. (2023). QSAR, molecular docking, and molecular dynamics simulation-based design of novel anti-cancer drugs targeting thio-redoxin reductase enzyme. *Structural Chemistry*. <https://doi.org/10.1007/s11224-022-02111-x>
- Faisal, S., Badshah, S. L., Kubra, B., Sharaf, M., Emwas, A.-H., Jaremko, M., & Abdalla, M. (2022). Identification and inhibition of the druggable allosteric site of SARS-CoV-2 NSP10/NSP16 methyltransferase through computational approaches. *Molecules*, 27(16), 5241. <https://doi.org/10.3390/molecules27165241>
- Hollingsworth, S. A., & Dror, R. O. (2018). Molecular dynamics simulation for all. *Neuron*, 99(6), 1129–1143. <https://doi.org/10.1016/j.neuron.2018.08.011>
- Hu, X., Zeng, Z., Zhang, J., Wu, D., Li, H., & Geng, F. (2023). Molecular dynamics simulation of the interaction of food proteins with small molecules. *Food Chemistry*, 405(Pt A), 134824. <https://doi.org/10.1016/j.foodchem.2022.134824>
- Kaminski, G. A., Friesner, R. A., Tirado-Rives, J., & Jorgensen, W. L. (2001). Evaluation and reparametrization of the OPLS-AA force field for proteins via comparison with accurate quantum chemical calculations on peptides. *The Journal of Physical Chemistry B*, 105(28), 6474–6487. <https://doi.org/10.1021/jp003919d>
- Kandsi, F., Elbouzidi, A., Lafdil, F. Z., Meskali, N., Azghar, A., Addi, M., Hano, C., Maleb, A., & Gseyra, N. (2022). Antibacterial and antioxidant activity of *Dysphania ambrosioides* (L.) Mosyakin and clematis essential oils: Experimental and computational approaches. *Antibiotics*, 11(4), 482. <https://doi.org/10.3390/antibiotics11040482>
- Karakas, E., Simorowski, N., & Furukawa, H. (2011). Subunit arrangement and phenylethanolamine binding in GluN1/GluN2B NMDA receptors. *Nature*, 475(7355), 249–253. <https://doi.org/10.1038/nature10180>
- Katan, M., & Luft, A. (2018). Global burden of stroke. *Seminars in Neurology*, 38(2), 208–211. <https://doi.org/10.1055/s-0038-1649503>
- Lipinski, C. A., Lombardo, F., Dominy, B. W., & Feeney, P. J. (1997). Experimental and computational approaches to estimate solubility and permeability in drug discovery and development settings. *Advanced Drug Delivery Reviews*, 23(1–3), 3–25. [https://doi.org/10.1016/S0169-409X\(96\)00423-1](https://doi.org/10.1016/S0169-409X(96)00423-1)
- Liu, Z., Qiu, X., Mak, S., Guo, B., Hu, S., Wang, J., Luo, F., Xu, D., Sun, Y., Zhang, G., Cui, G., Wang, Y., Zhang, Z., & Han, Y. (2020). Multifunctional memantine nitrate significantly protects against glutamate-induced excitotoxicity via inhibiting calcium influx and attenuating PI3K/Akt/GSK3beta pathway. *Chemico-Biological Interactions*, 325, 109020. <https://doi.org/10.1016/j.cbi.2020.109020>
- Martin, Y. C. (2005). A bioavailability score. *Journal of Medicinal Chemistry*, 48(9), 3164–3170. <https://doi.org/10.1021/jm0492002>
- Muegge, I. (2003). Selection criteria for drug-like compounds. *Medicinal Research Reviews*, 23(3), 302–321. <https://doi.org/10.1002/med.10041>
- Norgan, A. P., Coffman, P. K., Kocher, J.-P. A., Katzmann, D. J., & Sosa, C. P. (2011). Multilevel parallelization of AutoDock 4.2. *Journal of Cheminformatics*, 3(1), 12. <https://doi.org/10.1186/1758-2946-3-12>
- Ononamadu, C. J., Abdalla, M., Ihegboro, G. O., Li, J., Owolarafe, T. A., John, T. D., & Tian, Q. (2021). *In silico* identification and study of potential anti-mosquito juvenile hormone binding protein (MJHBP) compounds as candidates for dengue virus—Vector insecticides. *Biochemistry and Biophysics Reports*, 28, 101178. <https://doi.org/10.1016/j.bbrep.2021.101178>

- PkCSM. (n.d). Retrieved November 19, 2022, from <https://biosig.lab.uq.edu.au/pkcsm/prediction>
- Radan, M., Djikic, T., Obradovic, D., & Nikolic, K. (2022). Application of *in vitro* PAMPA technique and *in silico* computational methods for blood-brain barrier permeability prediction of novel CNS drug candidates. *European Journal of Pharmaceutical Sciences*, 168, 106056. <https://doi.org/10.1016/j.ejps.2021.106056>
- Reeves, M. J., Bushnell, C. D., Howard, G., Gargano, J. W., Duncan, P. W., Lynch, G., Khatiwoda, A., & Lisabeth, L. (2008). Sex differences in stroke: Epidemiology, clinical presentation, medical care, and outcomes. *The Lancet*, 7(10), 915–926. [https://doi.org/10.1016/S1474-4422\(08\)70193-5](https://doi.org/10.1016/S1474-4422(08)70193-5)
- Ritchie, T. J., Ertl, P., & Lewis, R. (2011). The graphical representation of ADME-related molecule properties for medicinal chemists. *Drug Discovery Today*, 16(1–2), 65–72. <https://doi.org/10.1016/j.drudis.2010.11.002>
- Sonkusare, S. K., Kaul, C. L., & Ramarao, P. (2005). Dementia of Alzheimer's disease and other neurodegenerative disorders – Memantine, a new hope. *Pharmacological Research*, 51(1), 1–17. <https://doi.org/10.1016/j.phrs.2004.05.005>
- Temme, L., Frehland, B., Schepmann, D., Robaa, D., Sippl, W., & Wünsch, B. (2018). Hydroxymethyl bioisosteres of phenolic GluN2B-selective NMDA receptor antagonists: Design, synthesis and pharmacological evaluation. *European Journal of Medicinal Chemistry*, 144, 672–681. <https://doi.org/10.1016/j.ejmech.2017.12.054>
- Thakral, S., Yadav, A., Singh, V., Kumar, M., Kumar, P., Narang, R., Sudhakar, K., Verma, A., Khalilullah, H., Jaremko, M., & Emwas, A.-H. (2023). Alzheimer's disease: Molecular aspects and treatment opportunities using herbal drugs. *Ageing Research Reviews*, 88, 101960. <https://doi.org/10.1016/j.arr.2023.101960>
- Veber, D. F., Johnson, S. R., Cheng, H.-Y., Smith, B. R., Ward, K. W., & Kopple, K. D. (2002). Molecular properties that influence the oral bioavailability of drug candidates. *Journal of Medicinal Chemistry*, 45(12), 2615–2623. <https://doi.org/10.1021/jm020017n>
- Xu, Q., Hu, M., Li, J., Ma, X., Chu, Z., Zhu, Q., Zhang, Y., Zhu, P., Huang, Y., & He, G. (2022). Discovery of novel brain-penetrant GluN2B NMDAR antagonists via pharmacophore-merging strategy as anti-stroke therapeutic agents. *European Journal of Medicinal Chemistry*, 227, 113876. <https://doi.org/10.1016/j.ejmech.2021.113876>
- Yalcin, S. (2020). Molecular docking, drug likeness, and ADMET analyses of Passiflora compounds as P-Glycoprotein (P-gp) inhibitor for the treatment of cancer. *Current Pharmacology Reports*, 6(6), 429–440. <https://doi.org/10.1007/s40495-020-00241-6>
- Zothantluanga, J. H., Abdalla, M., Rudrapal, M., Tian, Q., Chetia, D., & Li, J. (2023). Computational investigations for identification of bioactive molecules from *Baccaurea ramiflora* and *Bergenia ciliata* as Inhibitors of SARS-CoV-2 M^{PRO}. *Polycyclic Aromatic Compounds*, 43(3), 2459–2487. <https://doi.org/10.1080/10406638.2022.2046613>